Fibers and Polymers 2022, Vol.23, No.11, 3126-3137
DOI 10.1007/s12221-022-0298-9

ISSN 1229-9197 (print version)
ISSN 1875-0052 (electronic version)

Research on Influence of Matrix Component on the Mechanical Behavior of Multiaxial Warp-knitted Composites

Jiawei Chen[1], Xiaoping Gao[1]*, Ke Zhao[2], and Wei Wu[1]

[1]*School of Light Industry and Textiles, Inner Mongolia University of Technology, Hohhot 010050, China*
[2]*School of Mechanical, Inner Mongolia University of Technology, Hohhot 010051, China*
(Received March 29, 2022; Revised May 6, 2022; Accepted May 19, 2022)

Abstract: The mass ratio of curing agent to epoxy resin is one of the important factors affecting the behavior of matrix and composites. In this paper, the solution of curing agent to epoxy resin with different mass ratio (0.25, 0.30, 0.35 and 0.40) was selected as matrix, quadriaxial warp-knitted fabric was selected as reinforcement, and the composites were manufactured by applying vacuum assisted film infusion. Then the tensile and bending behavior of the composites was experimentally investigated, and the curing degree and failure mechanism of the composites were analyzed with respect to the thermodynamic properties and the microscopic failure morphologies. The optimal mass ratio was obtained by applying nonlinear fitting and verified by experiment, and a mathematical model was derived to predict the relationship between the strength and the mass ratio. The results showed that the thermal stability, curing degree, tensile and bending strength of the specimens increase firstly and then decrease with increase of the mass ratio. According to the tensile and bending strength results, the optimum mass ratio were obtained as 0.31 and 0.33 by applying nonlinear fitting to the experiment data. The results could lay a theoretical foundation for optimizing the mass ratio of matrix components, and improve the strength of composites.

Keywords: Ratio of component, Tensile strength, Bending strength, Nonlinear fitting, Composites

Introduction

Multi-axial warp-knitted fabric (MWFs) are a very interesting class of composite reinforcements, which are fabricated from multiple layers of straight fiber bundles with different orientations stitched together through warp knitting procedure [1,2]. Composites reinforced with MWFs have superior strength due to straight fiber bundles and have a broad application [3,4]. The mechanical behavior of composites mainly depends on the properties and structure of reinforcement materials, matrix properties, and the interface strength between fiber and resin, etc. [5-10]. At present, many authors investigated the interface modification between fiber and matrix by adding nanoparticles to the matrix [11-14]. However, the researches on the influence of matrix components (ratio between curing agent and resin) are rarely involved so far.

The bisphenol A epoxy resins have more excellent performance and are widely used in resin matrix composites [15-17], compared with other thermosetting resins. The mass ratio of epoxy resin to curing agent will affect the mechanical behavior of composites, because they occur cross-linking reaction under certain pressure and temperature during the preparation process to form a three-dimensional (3D) network polymer [18-21]. Shahriari *et al.* [22] analyzed the effect of the composition ratio on the water and oxygen permeability of the material, and found that the composition ratio has a remarkable relationship with the crosslinking density. It affected the crosslinking density, the macromolecular structure of the material, the water and oxygen permeability properties and the mechanical properties of the samples. Santa *et al.* [23] investigated the chemo-resistivity and mechanical properties of composites at different crosslinking degree values and found that the crosslinking density of the matrix has a huge effect on the diffusion behavior, electrical properties and mechanical properties of the composites. Miki *et al.* [24] used Python programming to analyze the relationship between the matrix ratio of the dental composites and compared the properties of the samples. It found that there was a strong correlation between the matrix ratio and the curing temperature and the mechanical properties of the sample. Hua *et al.* [25] studied the mechanical behavior of the matrix at different ratios and found that the mechanical behavior of the matrix was increased firstly and then decreased when amine curing agent added into the bisphenol A epoxy resin. Ma *et al.* [26] found that crosslinking density has a certain influence on the thermomechanical properties of composites through molecular dynamics research on thermosetting resins. Jing *et al.* [27] investigated the curing kinetics between synthetic aromatic amine curing agent and epoxy resin and found that the mechanical behavior of matrix could be improved dramatically with the increase of crosslinking point and crosslinking density. Wang *et al.* [28] developed the cross-linking model between curing agent and epoxy resin and obtained the mass of matrix increased as the crosslinking density increasing, and the optimum ratio between curing agent and epoxy were predicted. Therefore, it is necessary to study the composition ratio in matrix to improve the mechanical behavior of composites.

*Corresponding author: gaoxp@imut.edu.cn

In this paper, the quadriaxial warp-knitted glass fabric was selected as reinforcement, and the solution of curing agent to epoxy resin with different mass ratio were used as matrix to prepare composites by Vacuum Assisted Resin Infusion (VARI) process. The effect of the mass ratio on the thermal stability and the curing degree of the specimens was analyzed, and then the tensile and bending behaviors of the composites were evaluated. The relationship between the mass ratio and the mechanical properties of composites was obtained. Finally, as far as the mechanical behavior of the specimen is concerned, the optimal mass ratio was obtained by nonlinear fitting and experimental verification. The mathematical model could be used to predict the relationship between the mass ratio and the mechanical properties of composites. The results will provide a guidance for exploring the relationship between the mass ratio and the mechanical behavior of composites and the reaction mechanism of bisphenol A epoxy resin and alicyclic amine curing agent.

Experimental

Materials

In this paper, the quadriaxial warp-knitted glass fabrics supplied by Taishan Fiberglass Inc. (China). The photographs and structural parameters of the MWF are shown in Figure 1 and listed in Table 1, respectively. The epoxy resin and curing agent supplied by No. 1 Advanced Materials Co., Ltd. are No.1-692-2A and No.1-692-2B, respectively. The properties are listed in Table 2.

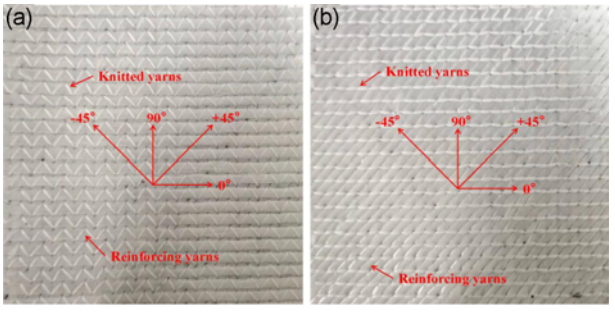

Figure 1. Photographs of MWF; (a) MWFs front and (b) MWFs back.

Composite Preparation

The composite panels were prepared by VARI process. The stacking sequence of MWF were $[0\ °/45\ °/90\ °/-45\ °]_4$. The mass ratio of curing agent to epoxy resin (The mass ration represents the mass fraction ratio between curing agent and epoxy resin in matrix solution) in the matrix were 0.25, 0.30, 0.35 and 0.40, respectively, and mixed uniformly. The process of VARI was shown in Figure 2.

Experiment

Thermal Stability

The thermal properties of the composite specimens with different mass ratio were characterized by thermogravimetric analysis (TGA) and differential scanning calorimetry (DSC) by STA 449 F5 Jupiter synchronous thermal analyzer. The test was performed over the temperature range of 25 °C to 700 °C in the atmosphere of N_2, with a heating rate of 10 °C/min and a flowing rate of 50 m//min. The relationship between the thermal stability and the mass ratio, and the curing degree of the specimens were also obtained.

Mechanical Properties

The tensile behavior of the specimens was tested using Shimadzu AGS-X universal strength machine according to ASTM D 3039. The size of the composite specimens was 250 mm×25 mm×2.5 mm, and at a speed of 2 mm/min. Three-millimeter-thick composite end tabs with dimension of 50 mm×25 mm was glued onto the samples to minimize localized damage and to provide better load transfer from the grips to the specimens, giving a gauge length of 150 mm. Five specimens were tested in each group. The tensile modulus was calculated based on the stress-strain curve using the secant modulus method.

The quasi-static three-point bending tests were performed on Shimadzu AGS-X universal strength machine at the speed of 1 mm/min according to ASTM D 7264. At least five groups are tested in each direction of the specimens and the average value is considered as the bending strength.

Table 1. Specifications of the multiaxial warp-knitted fabric

Structure	Axial	Yarn density (tex)	Layer	Weaving density (number/10 cm)	Mass (g/m^2)	Thickness (mm)
Quadriaxial	0 °	600	4	39	800	0.7
	45 °	300		55		
	90 °	300		40		
	-45 °	300		55		

Table 2. Physical properties of epoxy resin and curing agent

Material	Exterior (25 °C)	Viscosity (mPa·s, 25 °C)	Density (g/cm^3, 25 °C)	Epoxy equivalent (g/eq)
Epoxy resin NO.1-692-2A	Yellow clear viscous liquid	1000-2000	1.10-1.13	180-200
Curing agent NO.1-692-2B	Transparent clear liquid	10-20	0.9-0.95	-

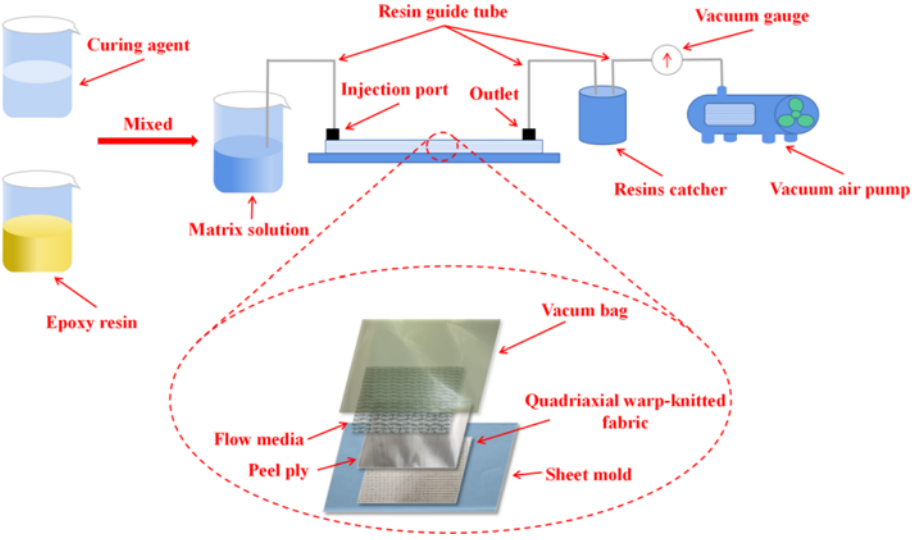

Figure 2. VARI process for composite preparation.

Damage Analysis

The fracture morphology of specimens with different mass ratio were observed using Bosheng BC1000 high-definition microscope and ApreoS LoVac electron microscope, and the effect of mass ratio on the mechanical properties of the composites was analyzed.

Results and Discussion

Effect of Mass Ratio on Thermal Stability of Compositess

Thermogravimetric Properties

Figure 3 shows the TGA curves of the compositess with different mass ratio. It shows that the thermal decomposition process of the specimens could be divided into three stages. When the temperature is below 340 °C, the specimens have a slight weight loss. Volatile substances begin to volatilize with the increase of temperature, resulting in a decrease of specimen quality. When the temperature ranges from 340 °C to 500 °C, the quality of specimens decreases rapidly as the temperature rising. The matrix begins to melt, and the stable macromolecular structure has been destroyed, so the matrix decomposed gradually. As the temperature rises over 500 °C, the quality of specimens tends to be stable, and the remaining glass fiber will not decompose.

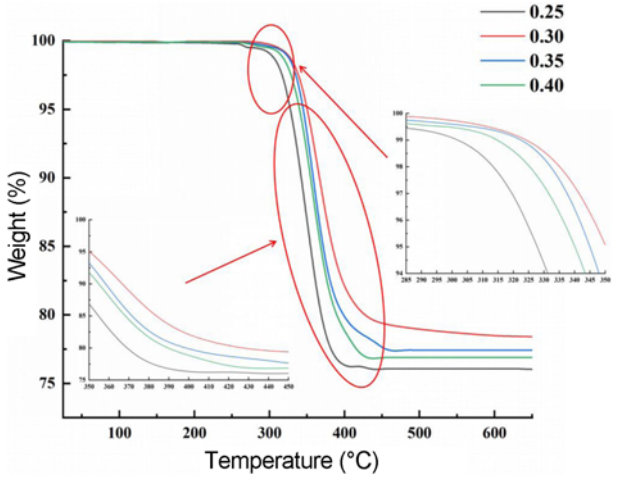

Figure 3. Thermal stability of specimens with different mass ratio.

The thermal stability of the composite specimens in this temperature range depends on the stability of the macromolecular structure of the matrix and the interface between the matrix and the fiber. The higher of the thermal stability of the specimens, the higher of the inflection point temperature of the thermal weight loss curve, and the higher of the stability of the macromolecular structure of the matrix and the interfacial stability between fiber and matrix. Compared with the mass ratio of 0.25, the inflection point of the weight loss curve of the sample increases by 26.48 °C when the mass ratio is 0.30. However, the inflection points decrease to the low temperature range as the mass ratio increased to 0.35 and 0.40. The reduction rates are 10.83 °C and 13.25 °C as the mass ratio are 0.35 and 0.40 in comparison to mass ratio of 0.30. Therefore, the specimen has the best thermal stability when the mass ratio is 0.30.

Curing Degree

The glass transition temperature (Tg) is the minimum temperature correspond to the movement of the molecular chain in specimens. The lower of the glass transition temperature, the higher of the content of flexible macromolecular chains in the matrix, and the lower of the curing degree of resin [28]. Therefore, the glass transition temperature of the specimens could be used to characterize the curing degree of resin at different mass ratio. The DSC curves of specimens with different mass ratio are shown in Figure 4. The glass

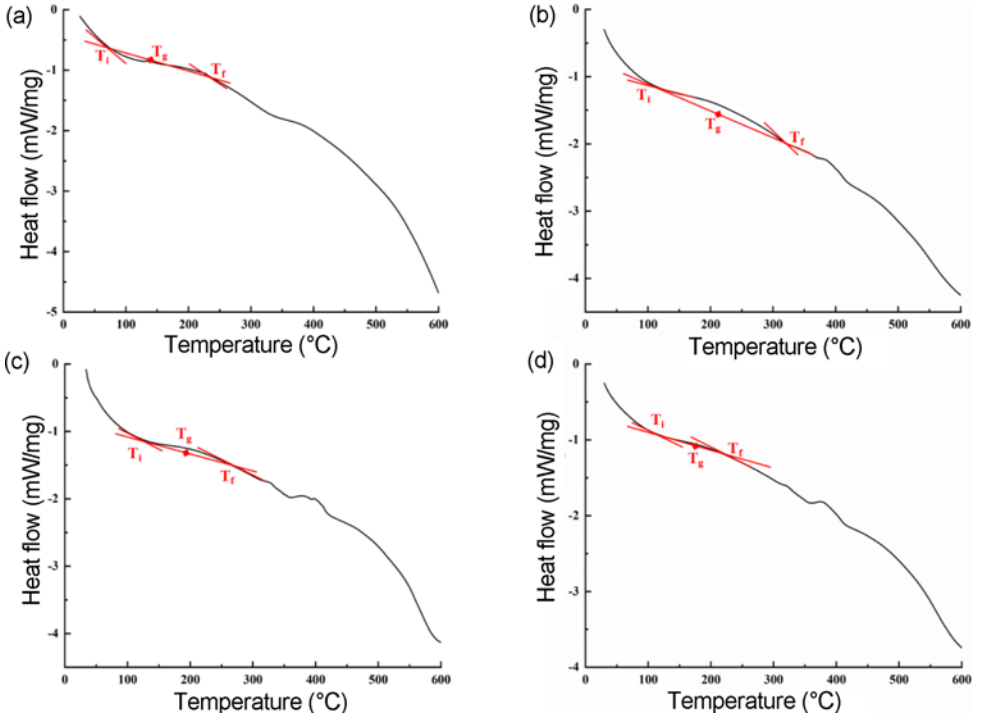

Figure 4. DSC curves of specimens with different mass ratio; (a) 0.25, (b) 0.30, (c) 0.35, and (d) 0.40.

Table 3. Glass transition temperature of specimens with different mass ratio

	Mass ratio between curing agent and epoxy resin			
	0.25	0.30	0.35	0.40
T_i (°C)	48.29	117.63	110.37	108.67
T_g (°C)	135.66	213.42	180.61	156.71
T_f (°C)	223.03	309.21	250.85	204.75

transition temperatures of specimens with different mass ratio were obtained by using the isometric method and shown in Table 3 (T_g is the glass transition temperature, T_i and T_f are the starting and ending temperatures of the glass transition, respectively).

As shown in Table 3, it can be concluded that the content of flexible macromolecules in the matrix system first decreased and then increased with the increase of mass ratio. The content of flexible macromolecules in the matrix system has the lowest value as the mass ratio is 0.30, and the matrix have the highest curing degree and the most stable molecular structure. The thermal stability of the specimens shows a trend of increasing firstly and then decreasing with the increase of mass ratio. The specimens have the best thermal stability as the mass ratio is 0.30.

Effect of Mass Ratio on the Mechanical Behavior of Composite

Tensile Properties

The stress-strain curves of tensile property of the specimens with different mass ratio in 0 °, 45 ° and 90 ° directions are shown in Figure 5. The tensile strength increases linearly with the strain increasing. As shown in Figure 5, it can be seen that the tensile strength has a maximum value when the mass ratio is 0.3.

Figure 6 and Table 4 show the tensile strength of specimens with different mass ratio in different directions. When the mass ratio ranges from 0.25 to 0.30, the tensile strength of the specimens in 0 °, 45 ° and 90 ° directions increase by 13.96 %, 12.14 % and 14.79 %, and the tensile modulus increases by 21.01 %, 24.69 %, 22.15 %, respectively. When the mass ratio is 0.35, the tensile strength of the specimens in 0 °, 45 ° and 90 ° directions increase by 4.21 %, 4.31 %, and 7.16 %, and the tensile modulus increases by 12.19 %, 8.92 %, and 8.68 %, respectively. When the mass ratio is 0.40, the tensile strength of the specimens in 0 °, 45 ° and 90 ° directions increase by 0.44 %, 1.20 %, and 1.75 %, and the tensile modulus increases by 1.69 %, 4.36 %, and 3.19 %, respectively.

Bending Properties

Figure 7 shows the stress-strain curves of bending properties of specimens with different mass ratio in 0 °, 45 ° and 90 ° directions. At the initial stage, the bending strength increases linearly with increase of strain, and the upper and lower surfaces of the specimens showed different degrees of damage. The bending failure of specimens showed different stages as the load increasing.

The bending strength of specimens with different mass ratio in 0 °, 45 ° and 90 ° directions are shown in Figure 8

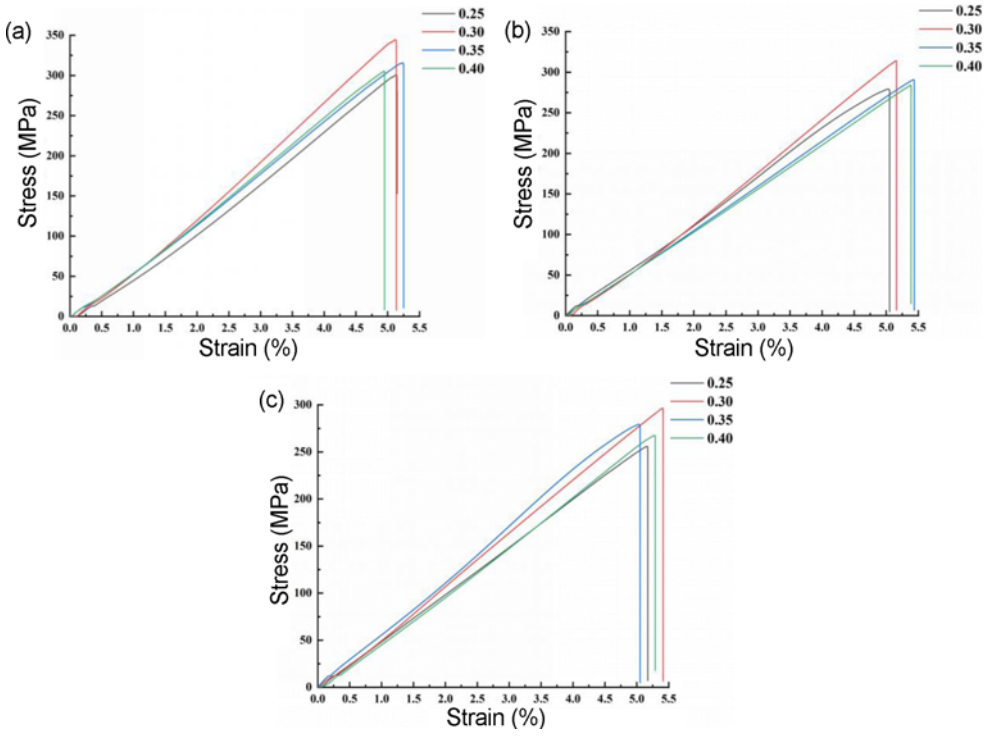

Figure 5. Tensile stress-strain curves; (a) 0 ° direction, (b) 45 ° direction, and (c) 90 ° direction.

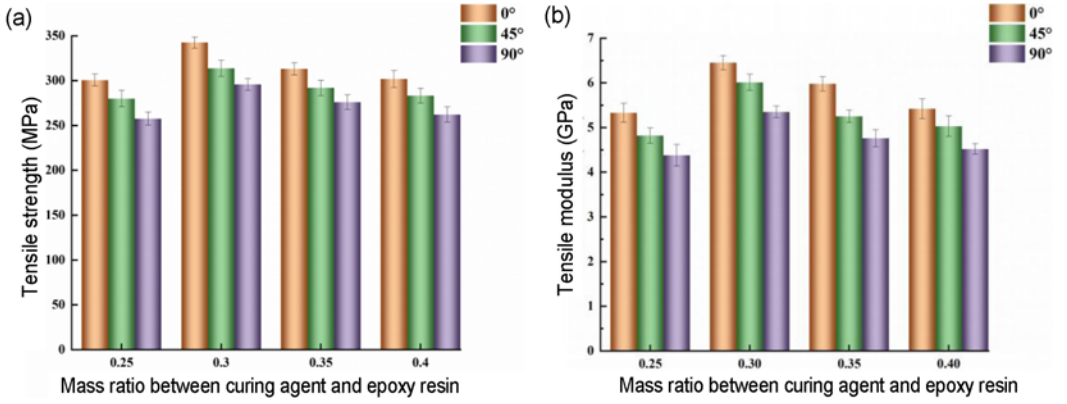

Figure 6. Comparison of tensile strength and modulus of specimens with different mass ratio.

and Table 5.

The matrix is the main bearing part when the specimen is subjected to bending load, so the mechanical properties of the matrix have a more significant effect on the bending properties of the composite than the tensile properties. When the mass ratio varies from 0.25 to 0.30, the 3D network structure inside the matrix is stable, and the mechanical properties of the matrix have been significantly improved. The bending strength increases by 33.99 %, 41.05 % and 41.01 % in 0 °, 45 ° and 90 ° directions, and the bending modulus increases by 36.68 %, 55.00 % and 50.05 %, respectively. When the mass ratio is 0.35, the 3D network structure inside the matrix began to be slightly damaged, and the mechanical properties of the matrix has been decreased. The specimens bending strength in 0 °, 45 °, and 90 ° directions increases by 21.78 %, 32.53 %, and 31.48 %, and the bending modulus increases by 28.96 %, 31.25 %, and 34.46 %, respectively. As the mass ratio is 0.40, the bending strength in 0 °, 45 °, and 90 ° directions increases by 18.89 %, 31.47 %, and 30.89 %, and the bending modulus increases by 20.75 %, 28.52 %, and 31.62 %, respectively.

Mechanism of Mechanical Behavior Variation

The crosslinking reaction diagram between epoxy resin and curing agent is shown in Figure 9. Firstly, the epoxy group in epoxy resin reacts with the primary amino group in curing agent to form a secondary amino group and linear

Table 4. Tensile behavior of composite specimens with different mass ratio

Mass ratio between curing agent and epoxy resin	Direction	Tensile strength (MPa)	Variety (%)	Tensile modulus (GPa)	Variety (%)
0.25	0 °	300.56±6.72	-	5.33±0.21	-
	45 °	279.89±9.29	-	4.82±0.17	-
	90 °	257.62±7.21	-	4.38±0.24	-
0.30	0 °	342.51±6.14	13.96↑	6.45±0.16	21.01↑
	45 °	313.88±9.03	12.14↑	6.01±0.18	24.69↑
	90 °	295.73±6.57	14.79↑	5.35±0.13	22.15↑
0.35	0 °	313.21±6.86	4.21↑	5.98±0.16	12.19↑
	45 °	291.96±8.57	4.31↑	5.25±0.14	8.92↑
	90 °	276.08±8.26	7.16↑	4.76±0.19	8.68↑
0.40	0 °	301.87±9.32	0.44↑	5.42±0.22	1.69↑
	45 °	283.25±8.28	1.20↑	5.03±0.23	4.36↑
	90 °	262.14±8.42	1.75↑	4.52±0.12	3.19↑

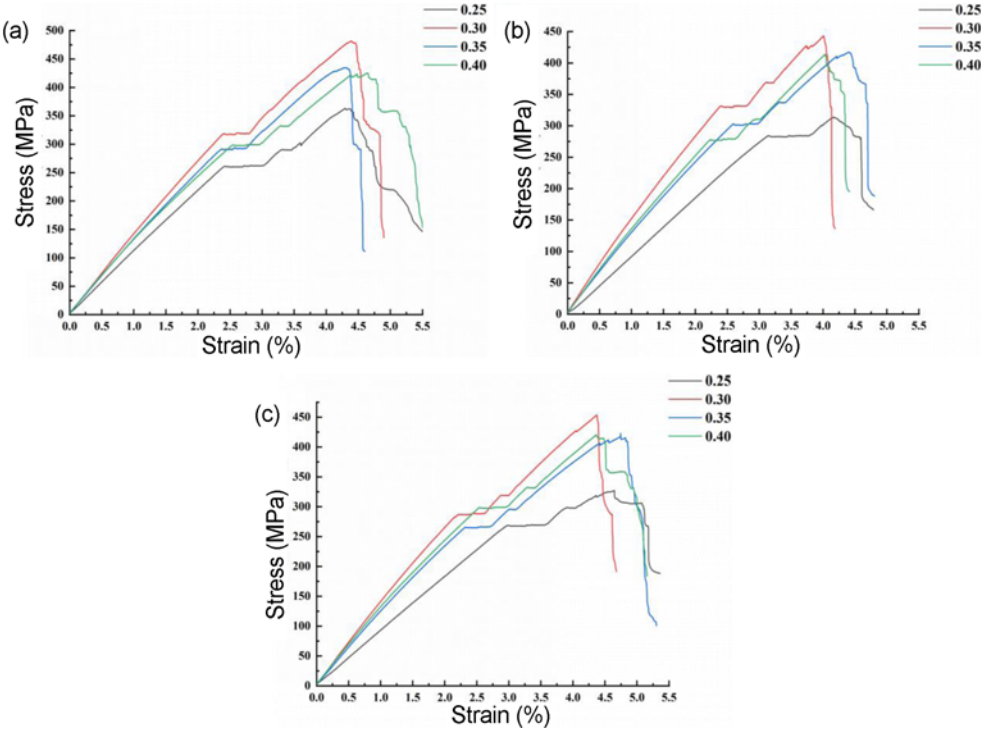

Figure 7. Bending stress-strain curves; (a) 0 ° direction, (b) 45 ° direction, and (c) 90 ° direction.

elastic macromolecule chain. Secondly, the generated secondary amine group reacts with the epoxy group to form a tertiary amine group, and the elastic macromolecule chain generates a rigid 3D network macromolecule.

When the content of curing agent in the matrix is insufficient, the number of cross-linking point in the matrix is lower and the uniformity is insufficient. It leads to the instability of the 3D network macromolecular structure, which in turn reduces the thermal stability, and the curing degree of matrix and the mechanical properties of specimens. With the increase of content of the curing agent, the number of cross-linking points in the matrix was increased, and the cross-linking density and uniformity were increased [30]. At this time, the 3D network macromolecules in the matrix tended to be structurally stable, and the mechanical properties, thermal stability of the specimens and the curing degree of the matrix were also increased. When the content of the curing agent is excessive, the relationship between

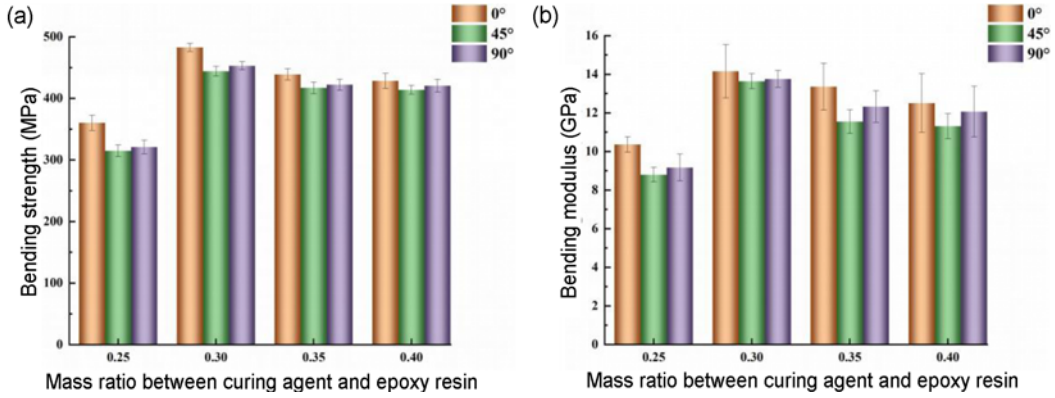

Figure 8. Comparison of bending strength and modulus of specimens with different mass ratio.

Table 5. Bending behavior of composite specimens with different mass ratio

Mass ratio between curing agent and epoxy resin	Direction	Bending strength (MPa)	Variety (%)	Bending modulus (GPa)	Variety (%)
0.25	0 °	360.38±12.33	-	10.36±0.40	-
	45 °	314.76±9.53	-	8.80±0.38	-
	90 °	321.10±11.26	-	9.17±0.69	-
0.30	0 °	482.88±6.60	33.99↑	14.16±1.38	36.68↑
	45 °	443.98±8.01	41.05↑	13.64±0.39	55.00↑
	90 °	452.79±6.58	41.01↑	13.76±0.44	50.05↑
0.35	0 °	438.89±9.16	21.78↑	13.36±1.21	28.96↑
	45 °	417.15±9.34	32.53↑	11.55±0.62	31.25↑
	90 °	422.18±9.05	31.48↑	12.33±0.82	34.46↑
0.40	0 °	428.47±12.15	18.89↑	12.51±1.52	20.75↑
	45 °	413.81±7.26	31.47↑	11.31±0.64	28.52↑
	90 °	420.56±10.34	30.98↑	12.07±1.31	31.62↑

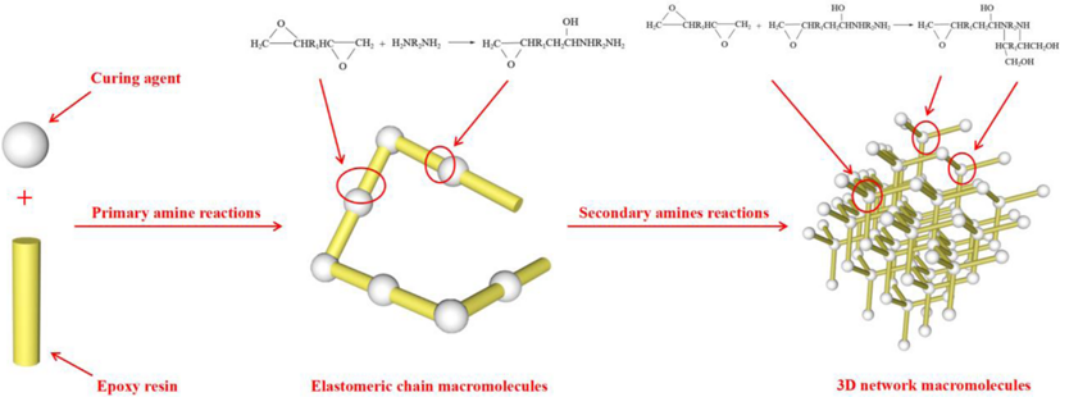

Figure 9. Schematic diagram of the principle of crosslinking reaction between epoxy resin and curing agent.

primary amine reaction and the secondary amine reaction is competitive relationship [31]. As a result, the length of the elastic macromolecules chain in the matrix system is increased, and the density of rigid cross-linking points in the system is decreased [32]. In turn, the stable structure of the 3D network macromolecules in the matrix is slightly

Table 6. Mechanical strength of specimens with different mass ratio

Strength	Direction	Mass ratio between curing agent and epoxy resin			
		0.25	0.30	0.35	0.40
Tensile strength (MPa)	0 °	300.56	342.51	313.21	301.87
	45 °	279.89	313.88	291.96	283.25
	90 °	257.62	295.73	276.08	262.14
Bending strength (MPa)	0 °	360.38	482.88	438.89	428.47
	45 °	314.76	443.98	417.15	413.81
	90 °	321.1	452.79	422.18	420.56

damaged, and the mechanical properties, thermal stability of specimens and the curing degree of the matrix are also decreased.

Fitting to Mechanical Strength

The mechanical behavior of composite specimens with different mass ratio in different directions are shown in Table 6. As far as the mechanical strength, the optimum mass ratio of the mechanical properties was obtained by applying nonlinear fitting to experimental data, as shown in Figure 10.

The obtained fitting equation could be used to predict the mechanical properties of quadriaxial warp-knitted glass

Table 7. Fitting constants for mechanical strength

Mechanical properties	Direction	Constants			Sum of squares of the correlation coefficients (R^2)
		A	B	C	
Tensile strength	0 °	6562.97	6.89	6.12	0.99
	45 °	5045.21	5.75	5.53	
	90 °	6271.69	7.61	6.38	
Bending strength	0 °	18561.82	13.74	7.93	0.98
	45 °	18209.78	14.73	7.95	
	90 °	18377.91	14.59	7.92	

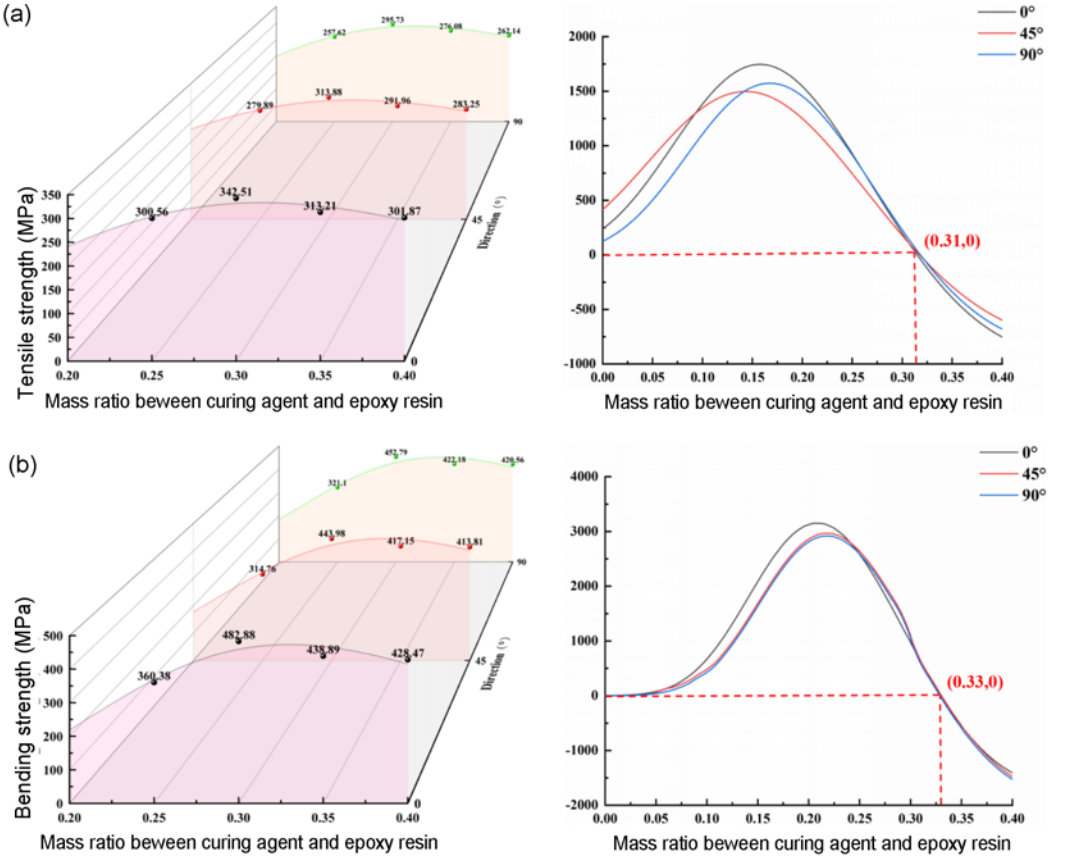

Figure 10. Fitting of the mechanical strength to mass ratio of curing agent and epoxy resin and its corresponding first derivative curve.

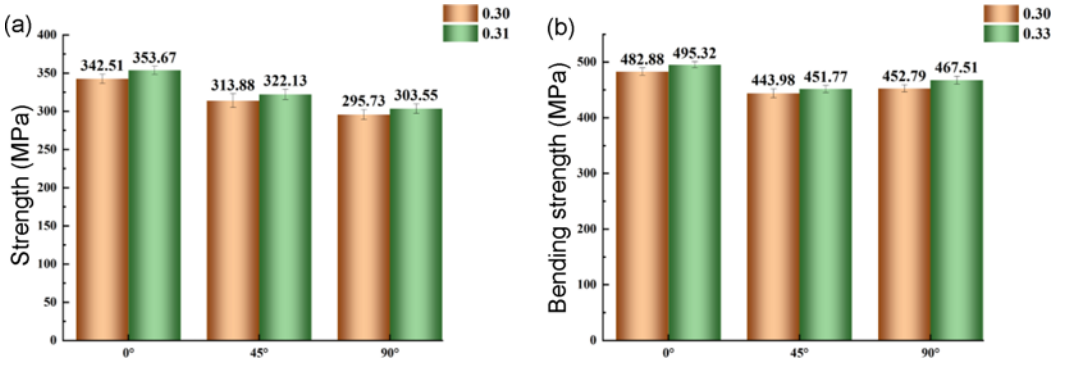

Figure 11. Comparison of mechanical strength between specimens with a mass ratio of 0.30 and optimum mass ratio.

composites according to the mass ratio of curing agent to epoxy. The fitting equation is as follows.

$$y = A\exp\left[-\frac{B}{\exp(Cx)} - Cx\right] \quad (1)$$

where, y is the mechanical strength, MPa, x is the mass ratio between curing agent and epoxy resin, A, B and C are constants.

As shown in Table 7, the squares sum of the correlation coefficients corresponding to tensile strength and bending strength of the specimens with different mass ratio in 0 °, 45 ° and 90 ° directions are 0.99 and 0.98, respectively. The theoretical curve has good agreement with the experimental one. Therefore, the fitted equation could be used to predict the variation of the mechanical property of composites with the mass ratio variation. After calculating the first derivative of the fitted curve, as shown in Figure 10, the optimal mass ratio corresponding to the tensile strength and bending strength of the specimens can be obtained as 0.31 and 0.33, respectively. In order to verify the accuracy of the fitted equation, the specimens with a mass ratio of 0.31 were prepared and tested for tensile strength in 0 °, 45 ° and 90 ° directions, and a mass ratio of 0.33 were prepared and tested for flexural strength in 0 °, 45 ° and 90 ° directions, as shown in Figure 11.

Therefore, the optimal mass ratio for tensile strength and flexural strength of the specimens are 0.31 and 0.33 on the basis of nonlinear fitting and experimental verification.

Fracture Morphology Analysis

Fracture Morphology in Macroscopic

Figure 12 shows the fracture morphology of the specimens in 0 ° direction. The relationship between the mass ratio and the tensile properties of the specimens was analyzed on the basis of the macroscopic fracture morphology. It can be seen that the tensile failure mode are fibers pull-out, fracture and

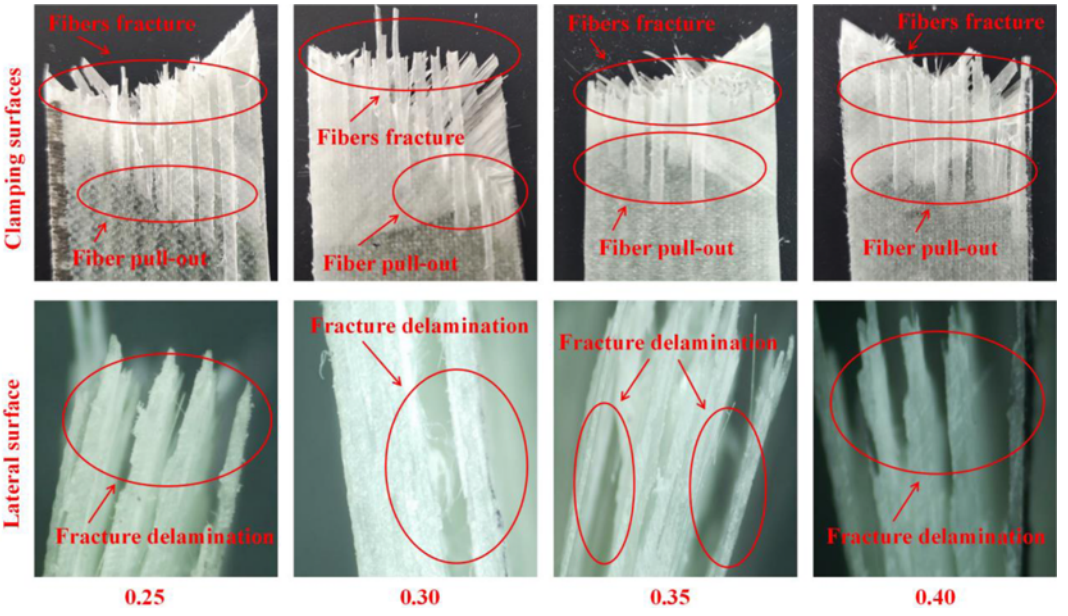

Figure 12. Tensile fracture morphology of the specimens in 0 ° direction.

delamination at the outer surface. As for mass ratio of 0.3, the specimens have uniform failure area and the delamination is not obvious, and the number of fractured matrix is small. As for mass ratio of 0.25, 0.35 and 0.40, the fibers at the outer surface of the specimens are obviously pulled out and the fracture mode is irregular. There is serious delamination in comparison to that of mass ratio of 0.3. Therefore, the properties of the matrix and the bonding strength between the matrix and the fiber are the best as the mass ratio is 0.30, and the tensile properties of the composites have the optimum value.

The flexural fracture morphologies of specimens with

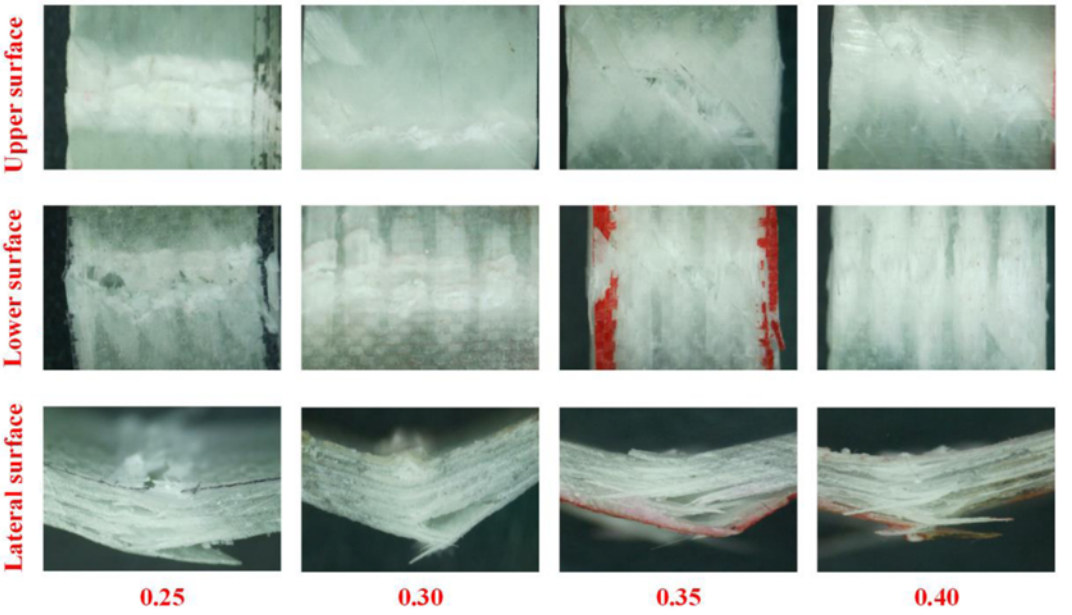

Figure 13. Bending fracture morphology of the specimens in 0 ° direction.

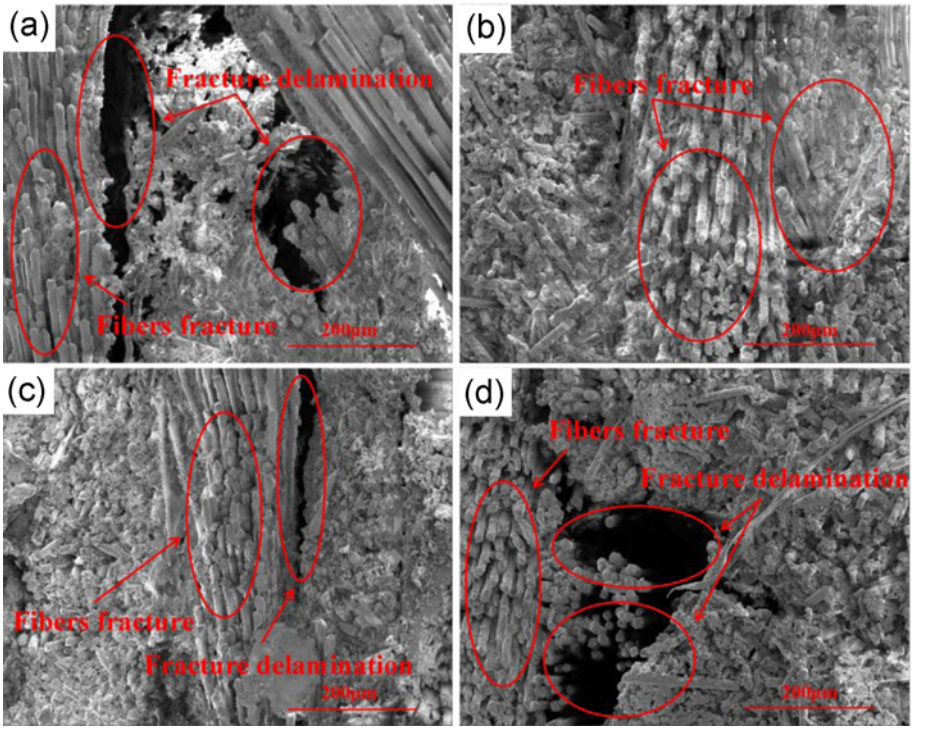

Figure 14. Fracture morphology of specimens with different mass ratio.

different mass ratios in 0 ° direction were observed by high-definition microscope, which could be used to analyze the relationship between the bending properties and the mass ratio at macro-scale. Figure 13 shows that the failure area is located at the place where the load applied, and damages appear on the upper and lower surfaces of the specimens. The specimen has the smallest damage as the mass ratio is 0.30. As the mass ratio is 0.25, 0.35 and 0.40, the damage of the specimen becomes serious, and there are more obvious delamination than that of mass ratio 0.30. The result shows that the properties of the matrix and the bonding strength between the matrix and the fiber are the best as for mass ratio of 0.30, and the bending properties have the optimum value.

Fracture Morphology Analysis in Microscopic

The influence of mass ratio on the mechanical properties of the specimens in 0 ° direction was analyzed in micro-scale, as shown in Figure 14. The fibers have more rougher surface as the mass ratio of 0.30, and the fibers are tightly bonded by matrix, and without obvious delamination between fiber and resin. As for mass ratio of 0.25, the fibers have smooth surface and serious delamination. Therefore, the specimens with mass ratio of 0.25 has the worst mechanical properties. The specimens with mass ratio of 0.35 and 0.4 both have obvious fiber delamination, compared with that of specimens with mass ratio of 0.30.

Conclusion

In this paper, the influence of mass ratio on the mechanical properties of quadriaxial warp-knitted glass fiber composites prepared with VARI process was studied. The conclusions are follows.

1. The mechanical properties, thermal stability and curing degree of the specimens shows a trend of increasing firstly and then decreasing with the increase of mass ratio between curing agent and epoxy resin.
2. The composite specimens have the optimum mechanical behavior as the mass ratio is 0.30. The tensile strength in 0 °, 45 ° and 90 ° directions is 342.51 MPa, 313.88 MPa and 295.73 MPa, respectively. The tensile modulus is 6.45 GPa, 6.01 GPa and 5.35 GPa, respectively. The flexural strengths in 0 °, 45 ° and 90 ° directions is 482.88 MPa, 443.98 MPa and 452.79 MPa, respectively. The flexural modulus is 14.16 GPa, 13.64 GPa and 13.76 GPa, respectively.
3. The optimal mass ratio corresponding to the tensile strength and flexural strength of the specimens are 0.31 and 0.33 by applying nonlinear fitting to the experimental results, which is also verified by the experimental data.
4. The curing mechanism between epoxy resin and curing agent was obtained. That is, the epoxy resin occurs primary amine reaction firstly and then secondary amine reaction to produce stable 3D network macromolecular structure. With the increase of curing agent content, the content of 3D network macromolecules is increased and the structure tends to be stable, and the performance of the specimens is improved. When the curing agent is excessive, the primary amine reaction and the secondary amine reaction compete with each other, which resulting in a slight damage to the 3D network macromolecular structure, and the performance of the specimens is decreased.
5. The bonding strength between fiber and epoxy resin is improved with the increase of mass ratio with respect to fracture morphology of specimen. However, the bonding strength between fiber and epoxy resin is decreased when the mass ratio exceeds 0.3. The mechanical behavior decreased and the rough fracture cross-section and the serious delamination are also observed.

Acknowledgment

The authors acknowledge the financial supports from the National Natural Science Foundation of China (Grant No. 51765051), the Postgraduate Scientific Research Innovation Project of Inner Mongolia (Grant No. S20210180Z) and the Natural Science Foundation of Inner Mongolia (Grant Nos. 2021MS01010 and 2020LH01001).

Conflict of Interest

We declare that we have no conflict of interest.

References

1. Z. Gao, G. Jiang, P. Ma, and S. Liu, *J. Text. Res.*, **34**, 144 (2013).
2. D. S. Lobanov and S. V. Slovikov, *Mech. Compos. Mater.*, **52**, 767 (2017).
3. Z. M. Huang, H. M. King, J. R. Youn, and Y. S. Song, *Fiber. Polym.*, **20**, 2665 (2019).
4. G. Mittal, K. Y. Rhee, V. M. Stanković, and D. Hui, *Compos. Part B-Eng.*, **138**, 122 (2018).
5. X. Gao, N. Tao, X. Yang, C. Wang, and F. Xu, *Compos. Part B-Eng.*, **159**, 173 (2019).
6. J. Novotna, V. Baheti, B. Tomkova, J. Militky, and J. Novak, *Fiber. Polym.*, **19**, 1288 (2018).
7. N. Tian, S. Wu, G. Han, Y. Zhang, Q. Li, and T. Dong, *J. Hazard. Mater.*, **424**, 127393 (2022).
8. J. Xi, J. Yu, and Z. Yu, *Fiber. Polym.*, **20**, 1301 (2019).
9. X. Pei, B. Shang, C. Li, J. Liu, and Y. Tang, *Compos. Part B-Eng.*, **91**, 296 (2016).
10. T. Dong, Q. Li, N. Tian, H. Zhao, Y. Zhang, and G. Han, *J. Hazard. Mater.*, **417**, 126133 (2021).
11. C. Wang, X. Gao, and Y. Li, *Fiber. Polym.*, **20**, 1495 (2019).
12. F. Chen, X. Liu, S. Li, S. Li, S. Li, T. Sun, Y. Zhao, and K.

Wang, *High. Perform. Polym.*, **34**, 292 (2022).
13. G. Withers, Y. Yu, V. Khabashesku, L. Cercone, V. Hadjiev, J. Souza, and D. Davis, *Compos. Part B-Eng.*, **72**, 175 (2015).
14. X. Luo, K. Yu, and K. Qian, *High. Perform. Polym.*, **30**, 803 (2018).
15. E. Mouri and M. Moriyama, *Fiber. Polym.*, **18**, 2261 (2017).
16. W. Shang and H. Jiang, *High. Perform. Polym.*, **32**, 793 (2020).
17. Y. Shi, T. Fu, Y. Xu, D. Li, X. Wang, and Y. Wang, *Chem. Eng. J.*, **354**, 208 (2018).
18. D. Zhang, Y. Xing, J. Bao, X. Zhong, and W. Liu, *Compos. Sci. Eng.*, **7**, 93 (2021).
19. Y. Li, Z. Zhou, X. Xu, and X. Long, *Adv. Mater. Res.*, **2203**, 3008 (2013).
20. X. Men, Y. Cheng, G. Chen, J. Bao, and J. Yang, *High. Perform. Polym.*, **27**, 497 (2015).
21. S. Aparna, D. Purnima, and R. Adusumalli, *Fiber. Polym.*, **19**, 1335 (2018).
22. L. Shahriari, M. Mohseni, and H. Yahyaei, *Prog. Org. Coat.*, **134**, 66 (2019).
23. S. Santa, K. Igors, S. Gita, and K. Maris, *Defect Diffus. Forum*, **6425**, 146 (2021).
24. H. Miki, F. Kotaro, H. Tadasuke, S. Hironao, U. Atsuko, K. Akiko, and K. Tatsushi, *Dent. Mater. J.*, **39**, 648 (2020).
25. Z. Hua, G. Liang, M. Lu, and X. Zhu, *New Chem. Mater.*, **50**, 180 (2022).
26. S. Ma, P. Chen, J. Xu, G. Chen, W. Min, and X. Xiong, *Ind. Eng. Chem. Res.*, **60**, 11621 (2021).
27. J. Qin, G. Zhang, R. Sun, and C. Wong, *J. Therm. Anal. Calorim.*, **117**, 831 (2014).
28. Z. Wang, Q. Lu, S. Chen, C. Li, S. Sun, and S. Hu, *Mol. Simul.*, **41**, 1515 (2015).
29. Y. Wang, W. Wang, G. Yang, Z. Zhang, and P. Li, *Polym. Compos.*, **42**, 6478 (2021).
30. B. Liang, G. Wang, X. Hong, J. Long, and N. Tsubaki, *High. Perform. Polym.*, **28**, 110 (2016).
31. N. Liu, Y. Bao, W. Zhou, Y. Zhang, and X. Zhang, *Synth. Mater. Aging Appl.*, **46**, 10 (2017).
32. B. Tang, X. Liu, X. Zhao, and J. Zhang, *J. Appl. Polym. Sci.*, **131**, 40611 (2014).